International Journal of Heat and Mass Transfer 52 (2009) 1458–1463

Contents lists available at ScienceDirect

International Journal of Heat and Mass Transfer

journal homepage: www.elsevier.com/locate/ijhmt

# Constructal design of T–Y assembly of fins for an optimized heat removal

Giulio Lorenzini [a,*], Luiz Alberto Oliveira Rocha [b]

[a] Department of Agricultural Economics and Engineering, Alma Mater Studiorum-University of Bologna, viale Giuseppe Fanin no. 50, 40127 Bologna, Italy
[b] Departamento de Física, Fundação Universidade Federal do Rio Grande, Cx.P. 474, Rio Grande, RS 96201-900, Brazil

ARTICLE INFO

Article history:
Received 3 April 2008
Available online 7 November 2008

Keywords:
Constructal design
Enhanced heat transfer
Fins
Optimization

ABSTRACT

Constructal design has been applied to a large variety of problems in nature and engineering to optimize the architecture of animate and inanimate flow systems. This numerical work uses this method to seek for the best geometry of a T–Y assembly of fins, i.e., an assembly where there is a cavity between the two branches of the assembly of fins. The global thermal resistance of the assembly is minimized by geometric optimization subject to the following constraints: the total volume, the volume of fin-material, and the volume of the cavity. Parametric study was performed to show the behavior of the twice minimized global thermal resistance. The results show that smaller cavity volume and larger fins volume improve the performance of the assembly of fins. The twice minimized global thermal resistance of the assembly and its corresponding optimal configurations calculated for the studied parameters were correlated by power laws.



## 1. Introduction

Constructal design [1–3] has been largely used to optimize flow systems in the engineering field [4–7]. This method is supported by Constructal law: "For a flow system to persist in time (to survive) it must evolve in such way that it provides easier and easier access to the currents that flow through it". The applicability of this law to the physics of natural and engineered flow systems has been discussed largely in the literature [2,3,7,8].

The design of fins with application to heat exchangers has been also documented in the literature [9,10]. The analysis of extended surfaces applying constructal design, however, is a recent fact. Bonjour et al. [11] studied analytically and numerically the geometrical optimization of radial and branched fins for a coaxial two-stream heat exchanger exploring the relationship between the performance and the architecture of the fins. Vargas et al. [12] conducted a three-dimensional study to optimize staggered arrangements of finned circular and elliptic tubes heat exchanger. This was an experimental and numerical work. It was calculated the optimal eccentricity, tube-to-tube and fin-to-fin spacing which maximizes heat transfer rate between a bundle of finned tubes in a given volume.

Bejan and Almogbel [13] optimized a T-shaped fin assembly. The objective was to maximize the global thermal conductance subject to total volume and fin-material constraints. Several configurations were studied: assemblies of plate fins and cylindrical fins, the tau-shaped assembly, and the umbrella-shaped construct using cylindrical fins. Their paper also shows a characteristic that is common to many optimized constructs: some geometrical features are relatively robust, i.e., insensitive to change in some design parameters. Lorenzini and Rocha [14] minimized the global thermal resistance subject to the total volume and fin material constraints to optimize a Y-shaped assembly of fins. This was a complete optimization, i.e., all the degrees of freedom were optimized and the optimized global thermal resistance and optimal shapes were correlated by power laws.

This work proposes the geometrical optimization of T–Y assembly of fins, i.e., an assembly where there is a cavity between the two branches of the assembly of fins. The objective is to minimize the global thermal resistance of the assembly subject to the total volume and the fin-material constraints, therefore the optimal configuration of the assembly of fins $[H_0/L_0,\ H_1/L_1]_{optimal}$ can be determined for the all the studied parameters.

## 2. Mathematical model

Consider the T–Y-shaped assembly of fins shown in Fig. 1. The configuration is two-dimensional, with the third dimension ($W$) sufficiently long in comparison with the height $H$ and the length $L$ of the volume occupied by the assembly of fins. The heat transfer coefficient $h$ is uniform over all the exposed surfaces. The heat current through the root section ($q_1$) and the temperature of the fluid ($T_\infty$) are known. The maximum temperature ($T_{max}$) occurs at the root section ($y = 0$) and varies with the geometry.

* Corresponding author. Tel.: +39 051 2096186; fax: +39 051 3762638.
E-mail addresses: giulio.lorenzini@unibo.it (G. Lorenzini), dfsrocha@furg.br (L.A.O. Rocha).

0017-9310/$ - see front matter © 2008 Elsevier Ltd. All rights reserved.
doi:10.1016/j.ijheatmasstransfer.2008.09.007

**Nomenclature**

| | |
|---|---|
| a | dimensionless parameter, Eq. (9) |
| $A$ | area [m$^2$] |
| $H$ | height [m] |
| $h$ | heat transfer coefficient [W m$^{-2}$ K$^{-1}$] |
| $k$ | fin thermal conductivity [W m$^{-1}$ K$^{-1}$] |
| $L$ | length [m] |
| $q$ | heat current [W] |
| $r$ | length of the root section [m] |
| $t$ | thickness [m] |
| $T$ | temperature [K] |
| $V$ | volume [m$^3$] |
| $W$ | width [m] |

*Greek symbols*

| | |
|---|---|
| $\alpha$ | angle between the tributary branches and the horizontal |
| $\theta$ | dimensionless temperature, Eq. (5) |
| $\phi$ | volume fraction of fin material |

*Subscripts*

| | |
|---|---|
| f | fin material |
| m | single optimization |
| mm | double optimization |
| o | optimal |
| oo | twice optimized |
| r | root ($H_r$ is the distance between the basis of the cavity and the wall) |
| 0 | cavity between the branches of the assembly |
| 1 | fin material |

*Superscript*

| | |
|---|---|
| (~) | dimensionless variables, Eqs. (6), (7), (10), (11), (14), (15) |

The objective of the analysis is to determine the optimal geometry ($H_0/L_0$, $H_1/L_1$, $H/L$) that is characterized by the minimum global thermal resistance $(T_{max} - T_\infty)/q_1$. According to the constructal design [3], this optimization can be subjected to two constraints, namely, the total volume (i.e., frontal area) constraint,

$$A = HL \tag{1}$$

and the fin-material volume constraint,

$$A_f = HL - 2L_1(H - H_1) - H_0L_0. \tag{2}$$

The cavity area located between the two branches of the assembly of fins is also considered constraint to diminish one degree of freedom of the assembly,

$$A_0 = H_0L_0. \tag{3}$$

Eqs. (2) and (3) can be expressed as the fin volume fraction

$$\phi_1 = A_f/A \tag{4}$$

and the cavity volume fraction

$$\phi_0 = A_0/A. \tag{5}$$

The analysis that delivers the global thermal resistance as a function of the assembly geometry consists to solve numerically the heat conduction equation along the T–Y-shaped assembly of fins where the fins are considered isotropic with constant thermal conductivity $k$,

$$\frac{\partial^2\theta}{\partial\tilde{x}^2} + \frac{\partial^2\theta}{\partial\tilde{y}^2} = 0 \tag{6}$$

where the dimensionless variables are

$$\theta = \frac{T - T_\infty}{q_1/kW} \tag{7}$$

and

$$\tilde{x}, \tilde{y}, \tilde{H}_0, \tilde{L}_0, \tilde{H}_1, \tilde{L}_1, \tilde{H}, \tilde{L} = \frac{x, y, H_0, L_0, H_1, L_1, H, L}{A^{1/2}}. \tag{8}$$

The boundary conditions are given by

$$-\frac{\partial\theta}{\partial\tilde{y}} = \frac{1}{\tilde{r}} \quad \text{at} \quad \tilde{y} = 0 \tag{9}$$

where $\tilde{r}$ is the dimensionless width of the root section and

$$-\frac{\partial\theta}{\partial\tilde{y}} = \frac{a^2}{2}\theta \quad \text{or} \quad -\frac{\partial\theta}{\partial\tilde{x}} = \frac{a^2}{2}\theta \quad \text{at the other surfaces.} \tag{10}$$

The parameter (a) that emerged in Eq. (10) was already used by Bejan and Almogbel [13] and defined as

$$a = \left(\frac{2hA^{1/2}}{k}\right)^{1/2} \tag{11}$$

The dimensionless form of Eqs. (1), (4), and (5) are

$$1 = \tilde{H}\tilde{L} \tag{12}$$

$$\phi_1 = \tilde{H}\tilde{L} - 2\tilde{L}_1(\tilde{H} - \tilde{H}_1) - \tilde{H}_0\tilde{L}_0 \tag{13}$$

$$\phi_0 = \tilde{H}_0\tilde{L}_0 \tag{14}$$

The maximal excess temperature, $\theta_{1,max}$ is also the dimensionless global thermal resistance of the construct,

$$\theta_{1,max} = \frac{T_{1,max} - T_\infty}{q_1/kW} \tag{15}$$

In the constructal design realm, the global thermal resistance or the global thermal conductance are used as performance indicator instead of the maximum fin efficiency. In this work we chose the global thermal resistance as performance indicator because we can get it directly from the temperature field calculated in the numerical simulation.

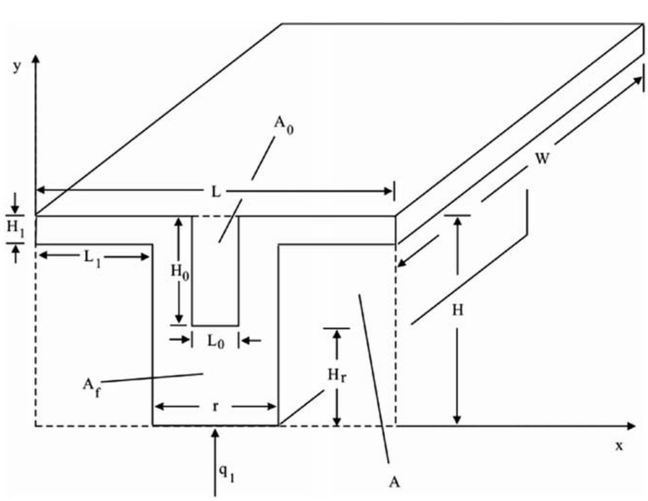


**Fig. 1.** Y–T-shaped assembly of fins analyzed.

## 3. Numerical model

The function defined by Eq. (15) can be determined numerically, by solving Eq. (6) for the temperature field in every assumed configuration ($H/L$, $H_0/L_0$, $H_1/L_1$), and calculating $\theta_{1,\max}$ to see whether $\theta_{1,\max}$ can be minimized by varying the configuration. In this sense, Eq. (6) was solved using a finite elements code, based on triangular elements, developed in MATLAB environment, precisely the PDE (partial-differential-equations) toolbox [15]. The grid was non-uniform in both $\tilde{x}$ and $\tilde{y}$, and varied from one geometry to the next. The appropriate mesh size was determined by successive refinements, increasing the number of elements four times from the current mesh size to the next mesh size, until the criterion $|\theta^j_{1,\max} - \theta^{j+1}_{1,\max}/\theta^j_{1,\max}| < 2 \times 10^{-4}$ was satisfied. Here $\theta^j_{1,\max}$ represents the maximum temperature calculated using the current mesh size, and $\theta^{j+1}_{1,\max}$ corresponds to the maximum temperature using the next mesh, where the number of elements was increased by four times. Table 1 gives an example of how grid independence was achieved. The following results were performed by using a range between 2,000 and 10,000 triangular elements.

To test the accuracy of the numerical code, the numerical results obtained using our code in Matlab PDE have been compared with the analytical results obtained by Bejan and Almogbel [13]. The domain in this case was a T-shaped assembly of fins ($\phi_0 = 0$). Table 2 shows that the two sets of results agree very well.

## 4. Optimal geometry

The numerical work consisted of determining the temperature field in a large number of configurations of the type shown in Fig. 1. Fig. 2 shows that there is an optimal ($H_1/L_1$) that minimizes the global thermal resistance when the parameters ($\varphi_0$,$\varphi_1$, and $a$) and the degrees of freedom ($H/L$, $H_0/L_0$) are fixed. This figure also shows that there is a second opportunity of optimization. Therefore, the results shown in Fig. 2 are summarized in Fig. 3, where the optimal ratio $(H_1/L_1)_o$ and the minimized maximal temperature, $(\theta_{1,\max})_m$, calculated in Fig. 2, are plotted as function of the ratio ($H_0/L_0$). The curve that represents $(\theta_{1,\max})_m$ in Fig. 3 indicates a shadow minimum when ($H_0/L_0$) is equal to 9.6. This twice minimized maximal temperature is named $(\theta_{1,\max})_{mm}$ and its value is 38.15. The corresponding optimal ratios are named $(H_0/L_0)_o$ and $(H_1/L_1)_{oo}$ and its values are also shown in Fig. 3. The subscript "o" means that the ratio ($H_0/L_0$) was minimized once, while the subscript "oo" means that the ratio ($H_1/L_1$) was minimized twice. The optimal ratio $(H_1/L_1)_o$ is approximately constant and equal to 0.07. Fig. 3 also shows that the optimal distance between the basis of the cavity and the wall ($\tilde{H}_r$)decreases when the ratio $H_0/L_0$ increases and the optimal value is equal 0.02, i.e., $\tilde{H}_r$ is optimal when the cavity penetrates almost entirely in the fin.

The procedure used in Figs. 2 and 3 is now repeated in Fig. 4 to illustrate the effect of the parameters $\phi_0$ and $\phi_1$ in the minimal global thermal resistance. This figure shows that $(\theta_{1,\max})_{mm}$ decreases when $\phi_0$ decreases and $\phi_1$ increases. This means that smaller cavities and larger fins improve the performance of the assembly of fins. Fig. 5 shows that the optimal ratio $(H_0/L_0)_o$ is almost insensitive to changes in the volume occupied by the fins, but it decreases when the volume of the cavity increases. The effect of the parameters $\phi_0$ and $\phi_1$ in the optimal ratio $(H_1/L_1)_{oo}$ is shown in Fig. 6. In general, $(H_1/L_1)_{oo}$ increases when $\phi_0$ and $\phi_1$ also increase. However, it increases more rapidly when $\phi_1$ is larger than 0.3. Fig. 7 shows that $(\tilde{H}_r)_{oo}$ does not depend on the volume occupied by the fins, but it decreases when the volume occupied by the cavity also decreases. This means that the smaller the value of $\phi_0$, the more the cavity penetrates in the fin and approximates to the wall.

Fig. 8 presents the effect of the parameter a in the optimal configuration when the aspect ratio of the assembly of fins, the volume occupied by the fins, and the volume occupied by the cavity are

**Table 1**
Numerical tests showing the achievement of grid independence ($\varphi_0 = 0.1$, $\varphi_1 = 0.2$, $a = 0.1$, $H/L = 1$, $H_0/L_0 = 9$, $H_1/L_1 = 0.07$)

| Number of elements | $\theta^j_{1,\max}$ | $\lvert((\theta^j_{1,\max} - \theta^{j+1}_{1,\max}))/\theta^j_{1,\max}\rvert$ |
|---|---|---|
| 141 | 38.3411 | $8.6069 \times 10^{-4}$ |
| 564 | 38.3741 | $5.0815 \times 10^{-4}$ |
| 2256 | 38.3936 | $1.8489 \times 10^{-4}$ |
| 9024 | 38.4007 | |

**Table 2**
Comparison between the results obtained using our MATLAB partial–differential-equations (PDE) toolbox code ($a = 0.1$, $\phi_1 = 0.2$, $\phi_0 = 0.00001$, $H/L = 0.0426$, $H_1/L_1 = 0.0154$, $H_0/L_0 = 1$). and the analytical results [2]

| | $L_1/L_0$ | $t_1/t_0$ | $q_{1,\max}$ |
|---|---|---|---|
| Analytical | 0.07 | 4.0 | 0.033 |
| Numerical | 0.07026 | 4.0041 | 0.03307 |

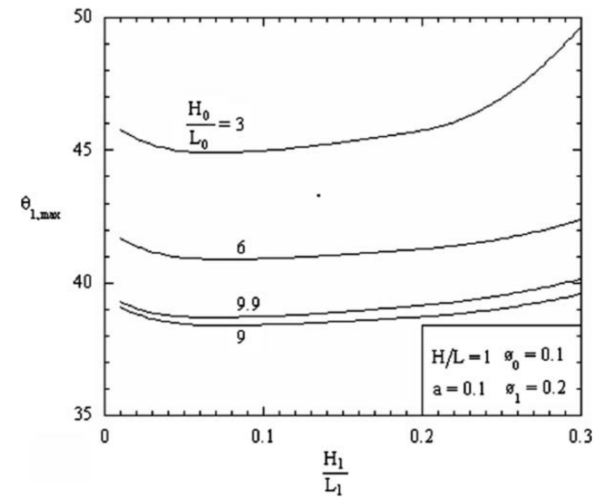


**Fig. 2.** The effect of $H_0/L_0$ and $H_1/L_1$ in the dimensionless maximal temperature.

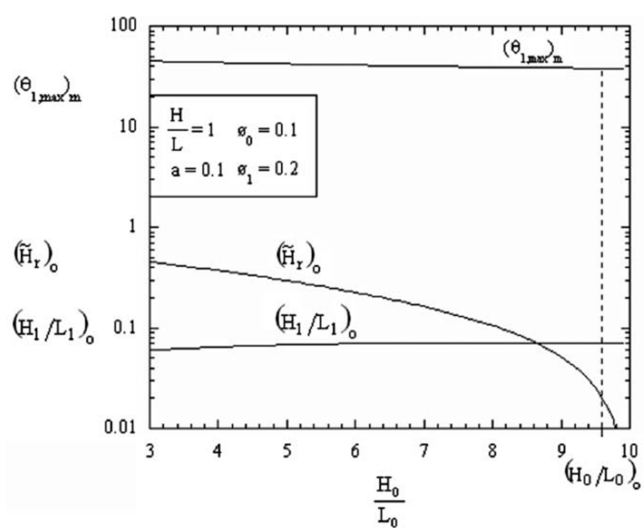


**Fig. 3.** The optimal results obtained in the first optimization.

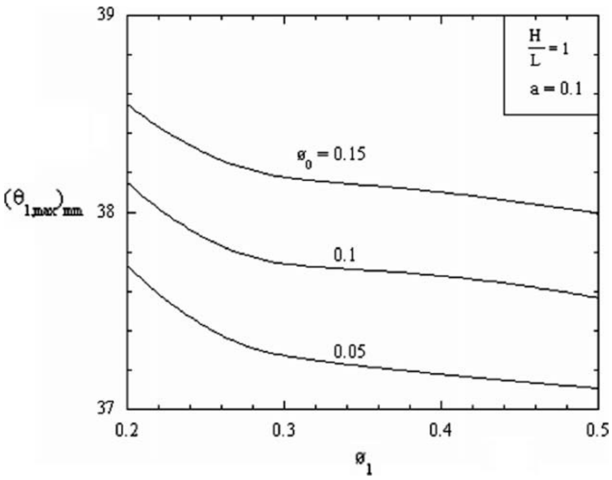


**Fig. 4.** The effect of $\phi_1$ and $\phi_0$ in the dimensionless minimal temperature optimized twice, $(\theta_{1,\max})_{mm}$.

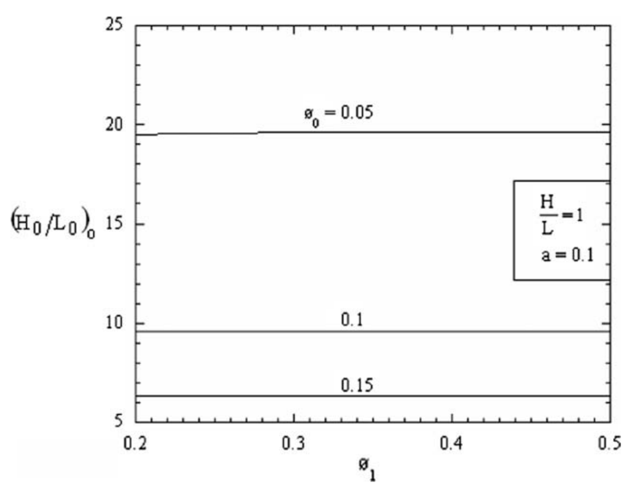


**Fig. 5.** The effect of $\phi_1$ and $\phi_0$ in the internal shape $(H_0/L_0)_o$.

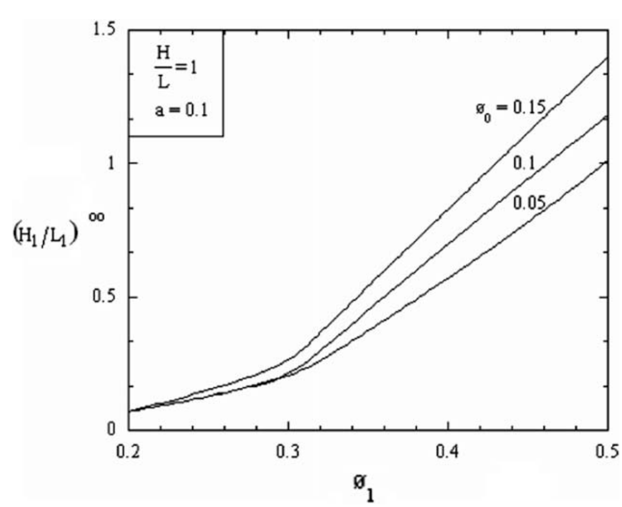


**Fig. 6.** The effect of $\phi_1$ and $\phi_0$ in the external shape $(H_1/L_1)_{oo}$.

fixed. This figure shows that the global thermal resistance decreases when a increase. This behavior was expected because it was already obtained by Bejan and Algmobdel [13] and Lorenzini and Rocha [14]. The optimal ratio $(H_1/L_1)_{oo}$ decreases when the value of a increases. $(H_0/L_0)_o$, however, is almost insensitive to changes in the value of a because it varies approximately 3.5% in the range of the studied a values. Eq. (16) correlates the global

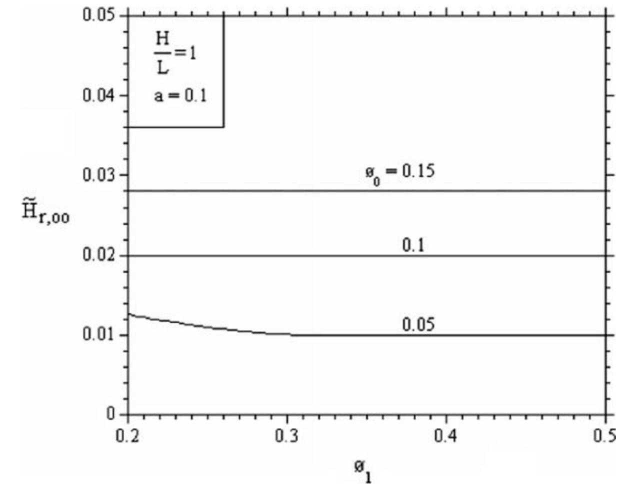


**Fig. 7.** The effect of $\phi_1$ and $\phi_0$ in the distance optimal distance $\tilde{H}_r$ .

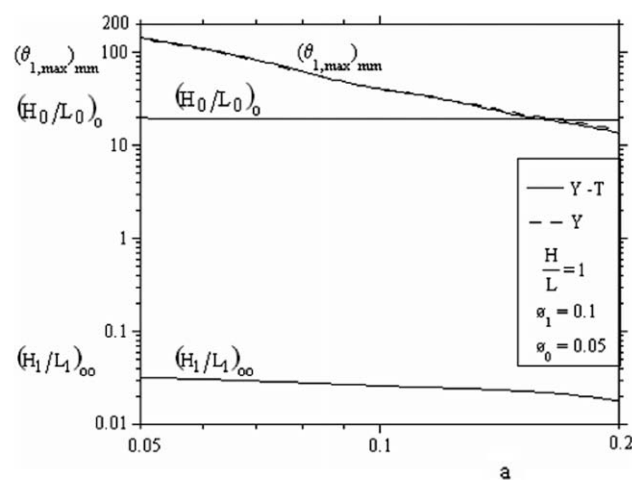


**Fig. 8.** The effect of the parameter a on the optimal shapes and performance.

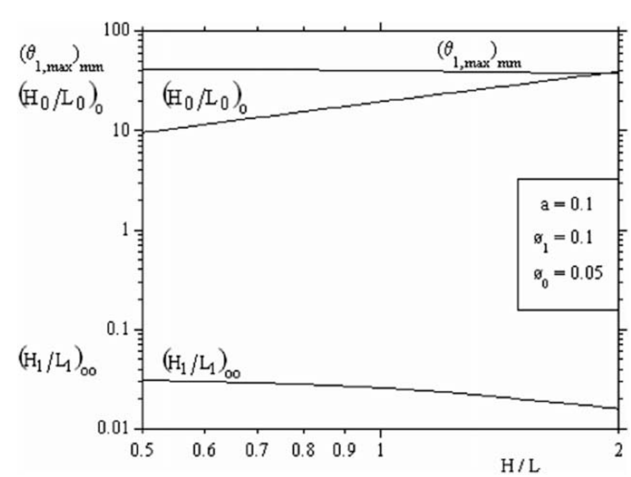


**Fig. 9.** The effect of the ratio $H/L$ on the optimal shapes and performance.

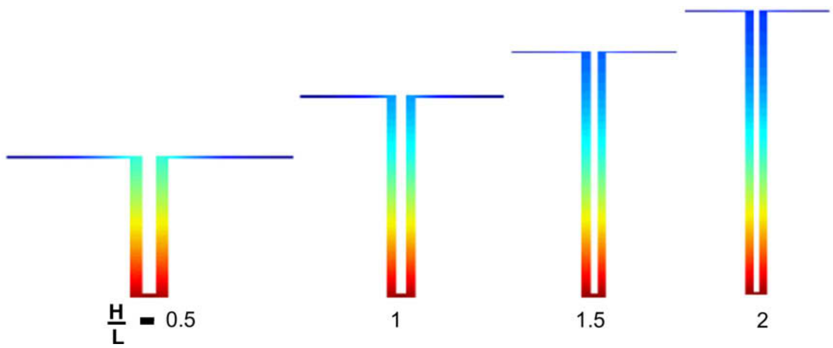


**Fig. 10.** The best configurations calculated in Fig. 9.

thermal resistance, $(\theta_{1,\max})_{mm}$, as function of the parameter a, the optimal ratio $(H_1/L_1)_{oo}$, and the optimal ratio $(H_0/L_0)_o$ within 1%,

$$(\theta_{1,max})_{mm} = 2.321 \times 10^{14} a^{-2.361} \left(\frac{H_0}{L_0}\right)_0^{-12.74} \left(\frac{H_1}{L_1}\right)_{oo}^{-0.812} \tag{16}$$

Eq. (16) is valid in the following ranges: $0.05 \leqslant a \leqslant 0.2$, $19 \leqslant (H_0/L_0)_o \leqslant 19.7$, and $0.018 \leqslant (H_1/L_1)_{oo} \leqslant 0.032$. The range $0.05 \leqslant a \leqslant 0.2$ was chosen to be consistent with practical values. Bejan and Almogbel [13] presented an example that could be applied to forced convection: the order of magnitude of $h$ is $10^2$ W/m$^2$ K, the thermal conductivities of aluminum and cooper are of order $10^2$ W/m K, and the length scale $A^{1/2} \sim 10^{-2}$ m results $a \sim 0.1$ in Eq. (11). Fig. 8 also compares the performance of the twice optimized Y–T-with the best Y-shaped assembly of fins as function of the parameter a. This figure shows that these configurations have similar performance, but the Y–T-assembly is slightly superior for values of $a \geqslant 0.1$ when $H/L = 1$. As will see in Fig. 9, the performance of this assembly increases as $H/L$ also increases which makes its performance superior to the Y-assembly of fins when $H/L > 1$. For example, if $a = 1$ and $\phi_1 = 0.1$, the best Y–T-shaped assembly of fins with $H/L = 2$ performs approximately 8% better than the optimized Y-shaped assembly of fins.

Fig. 9 shows that $(\theta_{1,\max})_{mm}$ and $(H_1/L_1)_{oo}$ decrease when the aspect ratio of the assembly of fins, $H/L$, increases. The optimal ratio $(H_0/L_0)_o$, however, is very sensitive to the changes in the ratio $H/L$ and increases when this ratio also increases. These optimal performance and configurations are correlated by Eq. (17) within 0.1%,

$$(\theta_{1,max})_{mm} = 31.27 \left(\frac{H}{L}\right)^{-0.2527} \left(\frac{H_0}{L_0}\right)_o^{0.214} \left(\frac{H_1}{L_1}\right)_{oo}^{0.1061} \tag{17}$$

Eq. (17) is valid in the following ranges: $0.5 \leqslant H/L \leqslant 2.0$, $9.5 \leqslant (H_0/L_0)_o \leqslant 39.2$, and $0.016 \leqslant (H_1/L_1)_{oo} \leqslant 0.031$.

The best configurations for several values of the aspect ratio $H/L$ calculated in Fig. 9 are shown in scale in Fig. 10.

## 5. Conclusions

This work presented the numerical optimization of a T–Y assembly of fins, i.e., an assembly where there is a cavity between the two branches of the assembly of fins. The dimensionless global thermal resistance was minimized by geometrical optimization subject to three constraints: the total volume, the fin material volume, and the cavity volume. The search for the best architecture was performed varying the two degrees of freedom that were ratios $H_0/L_0$, and $H_1/L_1$.

The double optimization showed the emergence of an optimal architecture $[(H_1/L_1)_{oo}, (\tilde{H}_r)_{oo}$ and $(H_0/L_0)_o]$ when the other parameters (a, $H/L$, $\phi_0$ and $\phi_1$) were fixed.

An important result is that the twice optimized global thermal resistance, $(\theta_{1,\max})_{mm}$, decreases when $\phi_0$ decreases and $\phi_1$ increases. This means that smaller cavities and larger quantity of fin material improve the performance of the assembly of fins.

It was also observed that the optimal distance between the basis of the cavity and the wall $(\tilde{H}_r)_o$ decreases when the ratio $H_0/L_0$ increases, and its optimal value occurs when the cavity penetrates almost totally in the fin. When it is optimized twice, $(\tilde{H}_r)_{oo}$ value does not depend on the volume occupied by the fins, but it decreases when the volume occupied by the cavity also decreases. This means that the smaller the value of $\phi_0$, the better the performance of the assembly of fins, and the more the cavity penetrates in the fin, i.e., its basis approximates to the wall.

Parametric study showed that the twice optimized global thermal resistance, $(\theta_{1,\max})_{mm}$ and the optimal ratio $(H_1/L_1)_{oo}$ decrease when the value of the parameter a increases. $(H_0/L_0)_o$, however, is almost insensitive to changes in the value of a. These optimal values were correlated within 1% by Eq. (16). $(\theta_{1,\max})_{mm}$ and $(H_1/L_1)_{oo}$ also decrease when the aspect ratio of the assembly of fins, $H/L$, increases. The optimal ratio $(H_0/L_0)_o$, however, is very sensitive to the changes in the ratio $H/L$ and increases when this ratio also increases. These optimal performance and configurations are correlated within 0.1% by Eq. (17).

## Acknowledgements

Prof. Giulio Lorenzini's work was sponsored by the Italian Ministry for Education, University and Research.

Prof. Luiz Rocha's work was sponsored by FAPERGS, Porto Alegre, RS, Brazil.

## References

[1] A. Bejan, Constructal-theory network of conducting paths for cooling a heat generating volume, International Journal of Heat and Mass Transfer 40 (1997) 799–816. published online 1 November 1996.
[2] A. Bejan, Advanced Engineering Thermodynamics, second ed., Willey, New York, 2007.
[3] A. Bejan, Shape and Structure from Engineering to Nature, Cambridge University Press, Cambridge, UK, 2000.
[4] J.V.C. Vargas, J.C. Ordóñez, A. Bejan, Constructal PEM fuel cell stack design, International Journal of Heat and Mass Transfer 48 (2005) 4410–4427.
[5] A. Bejan, N. Dan, Two constructal routes to minimal heat flow resistance via greater internal complexy, Journal of Heat Transfer 121 (1999) 6–14.
[6] L.A.O. Rocha, S. Lorente, A. Bejan, Constructal design for cooling a disc-shaped are by conduction, International Journal of Heat and Mass Transfer 45 (8) (2002) 1643–1652.
[7] A. Bejan, Constructal theory of pattern formation, Hydrology of Earth Systems Science 11 (2007) 753–768.
[8] A. Bejan, S. Lorente, The constructal law and thermodynamics of flow systems with configuration, International Journal of Heat and Mass Transfer 47 (2004) 3203–3214.

[9] A.D. Kraus, Developments in the analysis of finned arrays, in: Q. Donald, Kern Award Lecture, National Heat Transfer Conference, Baltimore, MD, August 11, 1997, International Journal of Transport Phenomena, 1 (1999) 141–164.
[10] A. Aziz, Optimum dimensions of extended surfaces operating in a convective environment, Applied Mechanics Reviews 45 (5) (1992) 155–173.
[11] J. Bonjour, L.A.O. Rocha, A. Bejan, F. Meunier, Dendritic fins optimization for a coaxial two-stream heat exchanger, International Journal of Heat and Mass Transfer 47 (1) (2004) 111–124.
[12] R.S. Matos, T.A. Laursen, J.V.C. Vargas, A. Bejan, Three-dimensional optimization of staggered finned circular and elliptic tubes in forced convection, International Journal of Thermal Sciences 43 (2004) 477–487.
[13] A. Bejan, M. Almogbel, Constructal T-shaped fins, International Journal of Heat and Mass Transfer 43 (2000) 2101–2115.
[14] G. Lorenzini, L.A.O. Rocha, Constructal design of Y-shaped assembly of fins, International Journal of Heat and Mass Transfer 49 (2006) 4552–4557.
[15] MATLAB, user's guide, version 6.0.088, release 12, The Mathworks Inc., 2000.